CBN 13-2
January 17, 2013

CHESS UPGRADE WITH COMBINED FUNCTION HARD BENDS

D.L.RUBIN & A. MIKHAILICHENKO, S. WANG, Y.LI

1. Introduction

The proposed rearrangement of the layout and optics in the CESR flares is the basis for a possible optimization of the storage ring for CHESS operation. By refitting the hard bends as combined function (vertically focusing) magnets and careful matching to the CESR arcs, it is possible to achieve relatively low emittance, and to accommodate as many as a total of six undulator beam lines. Changes to the CESR layout are limited to the region south of both east and west RF. The F and G lines are preserved. With the elimination of the horizontal separator in the east, the F line wiggler could be replaced with a 5 m long undulator. In the west, the RF could be translated a couple of meters to the south, making space for a 5 m undulator at G-line. There are additionally 4, 6 meter, zero dispersion straights, separated by 10^o of bend, between the west and east cavities, that could be fitted with undulators. The configuration is compatible with ongoing CesrTA low emittance program, as there is space for damping wigglers, as well as undulators in the zero dispersion straights. Horizontal emittance at 5.3GeV is 25 nm-rad, and at 2GeV with damping wigglers, $\epsilon_x \sim 1.5$ nm-rad.

2. Storage Ring Optics

In order to save space for undulators, vertical focusing is incorporated into the hard bends. The existing 8 hard bends, and the 2 each soft bends and quarter normal bends that together provide the 51.3^o of bend from west to east RF straights, are replaced with 10 equal strength combined function bends, with length $l = 3.238$ m (same as the existing hard bends), bending radius 35.97 m (as compared to $\rho = 31.65$) and $k = -0.1056\text{m}^{-2}$. The pole faces of the existing magnets can be modified to produce the required gradient as shown in Figure 1. (There remains the question of finding two additional hard bend magnets. Possibly, the combination of hard and soft bends in L3 can be replaced with normal bending magnets, so that the hard bends can be used in L0.)

Nine horizontally focussing quadrupoles are required, five very strong quadrupoles ($k = 1.29\text{m}^{-2}$, and $l = 60$cm), and four strong quadrupoles ($k = 0.62\text{m}^{-2}$, and $l = 60$cm) (For reference, existing CESR quadrupoles with copper coils can operate at $k = 0.62\text{m}^{-2}$ at 5.3

Date: January 17, 2013.

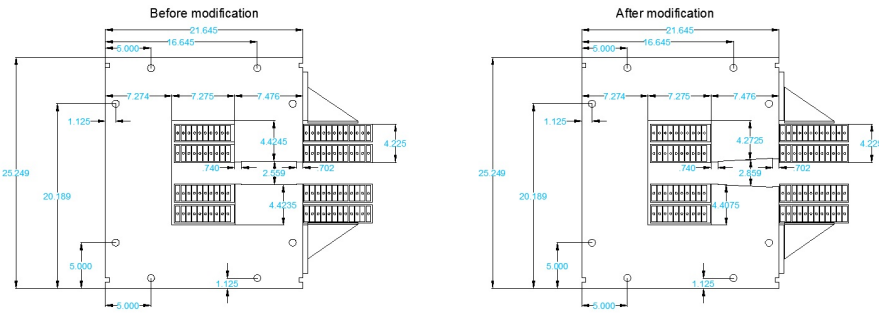

modification -2.jpg

FIGURE 1. The cross section of the hard bend dipole is shown on the left, and with the pole face modified to provide a vertically focusing gradient on the right.

GeV, but probably not at 6.5GeV. We plan to build a longer (1 m quadrupole) , for the very strong quadrupoles described above using the inventory of Mark II quad laminations in the warehouse to lengthen existing 60cm quadrupoles.)

The layout and optical functions extending from Q10W at the left to Q10E at the right, are shown in Figures 2 and 3.

The match to the arcs is shown in the plot of the twiss parameters for the entire ring in Figure 4. A consequence of the requirement that there be zero dispersion through the RF straights, is that the dispersion is relatively high in the nearby arc bends (B10-B15). Recall that bend 14 was removed to make space for wigglers, and coils added to B13 and B15 to compensate for the missing magnet. The result is high dispersion in high field bending magnets which makes a significant contribution to the emittance. So for the purposes of this design exercise we assume that bend 14 has been restored. The lattice parameters are summarized in Table 1. The lengths of the drifts in the reconfigured hard bend region can easily be adjusted to preserve the ring circumference.

3. Dynamic Aperture

Sextupoles are powered in two families to correct chromaticity to unity in both planes. Dynamic aperture is shown in Figure 5 for an on energy trajectory and $\pm 1\%$ off energy. The dashed lines correspond to the physical space required by a particle with total horizontal and vertical amplitude of 10, 20, and $30\sigma_x$ respectively, where σ_x assumes $\epsilon_x = 25.5$ nm-rad. The dynamic aperture is clearly more than adequate.

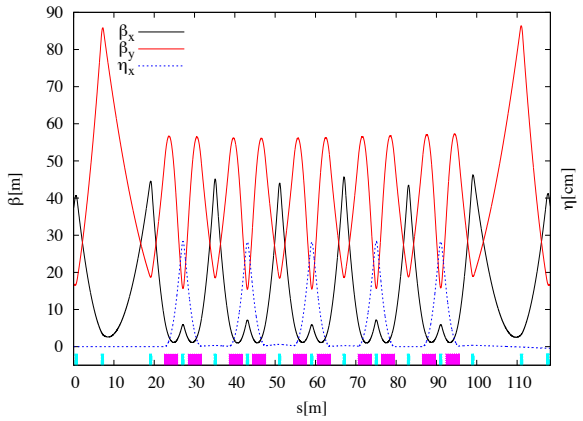

FIGURE 2. Optical functions through L0. The light blue rectangles represent quadrupoles and the purple, combined function bending magnets. The quadrupole at 0 is Q10W. Q09W is next at about 7m. The g-line wiggler and then the RF are just to the right of Q09W. Similarly, the rightmost quadrupoles are Q09E and Q10E. There is zero dispersion in the RF straights, and zero dispersion in the four straight sections between the pairs of bends. Vertical beta is relatively high in the undulator straights, but in view of the small emittance, probably OK even with a 5 mm gap. Or we might reduce the peak vertical beta by increasing the focusing strength of the bends or adjusting the lengths of the drifts between bends and quadrupoles.

4. Error tolerance

We have grown accustomed to the flexibility afforded by independent control of all of the storage ring quadrupoles. By including the vertical focusing as part of the bends we can no longer correct focusing errors by simply adjusting the appropriate quad. Furthermore, we are unable to trim the hard bends with backleg windings, to correct the orbit, as any change in field will also change focusing. But the relatively high density of horizontal quadrupoles provides significant leverage for compensating nearby errors. Indeed, the density of adjustable quadrupoles is no different than in the existing layout. We have shown that the lattice can be readily adjusted by varying the quadrupoles, to compensate the focusing of six 1.9T damping wigglers at 2.085 GeV, as shown in Figure 3. A more detailed analysis of error tolerance is required to determine how many corrector magnets (dipole and possibly quadrupole) are needed. We are also investigating the possibility of including trim winds on the pole faces of the hard bend magnets for fine adjustment of dipole, quadrupole and sextupole components.

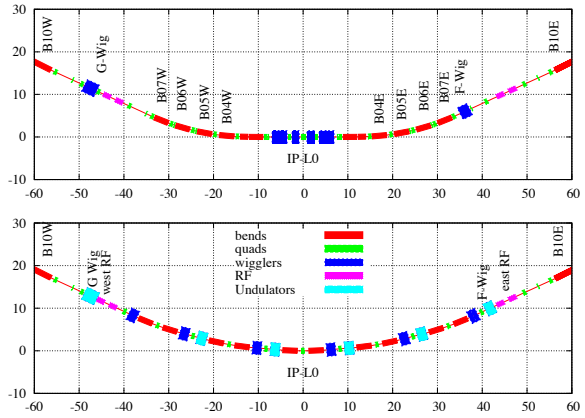

FIGURE 3. L0 layout. At the top is the existing layout from Q10W to Q10E. G-line and F-line wigglers are indicated, as are the superconducting damping wigglers . The bottom figure shows the proposed layout including additional undulators. The G-line wiggler remains undisturbed in the west. (The RF cavities, also undisturbed, are shown in pink.) Radiation from the blue "wigglers" (or undulators) at about 40m is directed down the existing F-line. Four additional 2 meter undulators are shown. The undulatory between 20-30m will correspond most closely to D-line. There is zero horizontal dispersion in all of the insertion straights. (Beam goes from right to left)

5. Electron cloud

We have assumed all beam lines see photons from a beam traveling in the clockwise direction, the positron direction. Total beam current and vertical emittance will likely be limited by the relatively high density electron cloud that evolves in the CESR aluminum vacuum chambers. The electron cloud can be mitigated by coating all of the CESR bend chambers with titanium-nitride. Coating the chambers would also benefit the CesrTA program, extending our ability to investigate electron cloud physics to the high intensity regime. Alternatively, we can reverse all magnets in synchrotron and CESR (and a few in the linac) and circulate electrons in the clockwise direction.

6. Wigglers

Note that each zero dispersion straight is split by a quadrupole into two 3.45 m drifts. One could imagine placing a 3 meter long undulator in one of the drifts, and a superconducting wiggler in the other. The wigglers could be used for ultra-low emittance operation for CesrTA or possibly for low energy operation of CHESS. In summary, the lattice can

TABLE 1. Lattice parameters (Values in parenthesis are with 11 damping wigglers at 1.3T for 2.1GeV and 1.9T for all other energies.) Note that (Beam Power [kW]) = (Energy Loss/Turn[MeV]) X (Beam Current [mA]) where Beam Power refers to the synchrotron radiation power only.

Energy[GeV]	5.289	3.0	6.5	2.1
ϵ_x[nm-rad]	25.5(13.0)	8.3(3.0)	38.8(23.5)	4.0(1.5)
ϵ_y[pm-rad]	50(25)	10(5)	60(40)	2(2)
Current [mA]	500	500	200	500
Bunches	600	600	600	600
Q_x	15.86	15.86	15.86	15.86
Q_y	7.26	7.26	7.26	7.26
Q_z	0.0364	0.0484	0.0328	0.0579
Acc. Voltage [MV]	6	6	6	6
τ_x[ms]	24(12)	133(32.2)	13(7.8)	388(97.2)
τ_y[ms]	27(12.6)	146(33.0)	14(8.3)	427(99.5)
τ_z[ms]	14(6.5)	78(16.7)	7.6(4.3)	226(5.0)
α_p	5.7×10^{-3}	5.7×10^{-3}	5.7×10^{-3}	5.7×10^{-3}
$\sigma_E/E[\times 10^{-4}]$	6.2(10.9)	3.5(9.3)	7.5(11.5)	2.4(6.4)
σ_l[mm]	11.8(20.9)	5(13.4)	16.0(25.4)	2.9(7.7)
Energy loss/turn [MeV]	1.0(2.)	0.1(0.47)	2.3(4.0)	0.025(0.11)
Beam Power [kW]	500(1000)	50(235)	460(800)	12.5(55)
Circumference [m]	768.438	768.438	768.438	768.438

accommodate as many as 6 undulators and 6 superconducting wigglers in L0 in addition to the 6 wigglers now in the arcs.

7. Beam lines

Figure 6 shows the existing layout of magnets and beam lines, as well as the proposed layout. The bends and quads in the new layout are outlined in red and blue respectively. The west and the end of the east RF cavities are visible.

In Figure 7 a solid black line indicates the X-ray beam line for the undulators, (excepting F and G) shown schematically in Figure 3. The length of the black lines corresponds to the distance from the F-line wiggler to the back wall of the F2 hutch. Apparently no significant civil construction is required for beam lines equivalent to F2. Indeed, the new F-line, as well as the line clockwise next to F could be made somewhat longer than at present. The existing CESR hard bend magnets have been omitted in Figure 7.

8. Effort

(1) Replace east and west hardbend/softbends in L3 with standard chevron.
(2) Restore B14 east and west
(3) Remove magnets and vacuum chambers from west to east RF

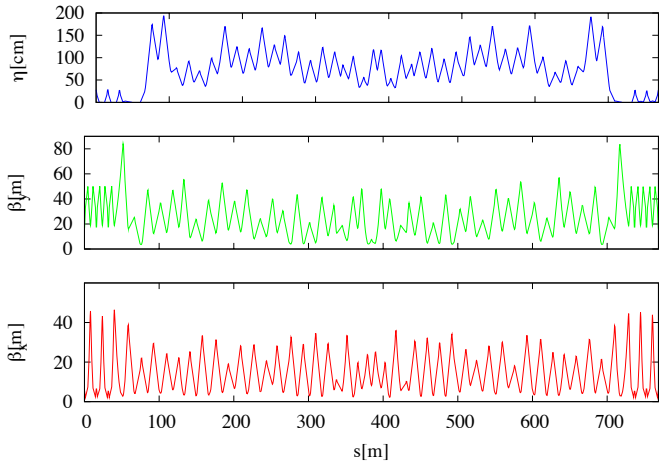

FIGURE 4. Twiss parameters for the entire ring. The very center of L0 is at $s = 0$ in the plot. The west flare extends from 0 to 60 meters, and the east flare from 710 to 768 meters. Note the relatively high dispersion in the arc bends adjacent to the zero dispersion RF straight (60-100m, and 670-710m). In this design we assume that B14 has been restored.

(4) Modify poles of 10 hard bend magnets for suitable gradient
(5) Build 5 100cm quadrupoles by adding laminations to existing 60cm magnets and purchase coils.
(6) New vacuum chamber through L0, including crotches, and coated with TiN to suppress electron cloud using extrusions that are in our warehouse.
(7) Install new quadrupoles, modified hard bends, vacuum chamber, etc. through L0
(8) 3-4 new x-ray beam lines, hutches, etc.

9. CesrTA

As shown in Table 1, the proposed configuration yields horizontal emittance of 1.5 nm-rad at 2.1 GeV assuming 11 wigglers operating at 1.3T. This compares to 2.5 nm-rad in the current CesrTA low emittance optics where we use 12 wigglers at 1.9T. In addition to the smaller horizontal emittance, the energy spread is reduced in the new layout from 0.081% to 0.064% and the bunch length from 10.6 mm to 7.7 mm, as a result of the lower wiggler field. Furthermore, as there is zero dispersion in the RF cavities, coupling of longitudinal and transverse motion is much smaller than in the standard CesrTA optics. In fact, in the current conditions, due to the approximately 1m horizontal dispersion in the RF cavities, the projected horizontal emittance is more than twice the normal mode

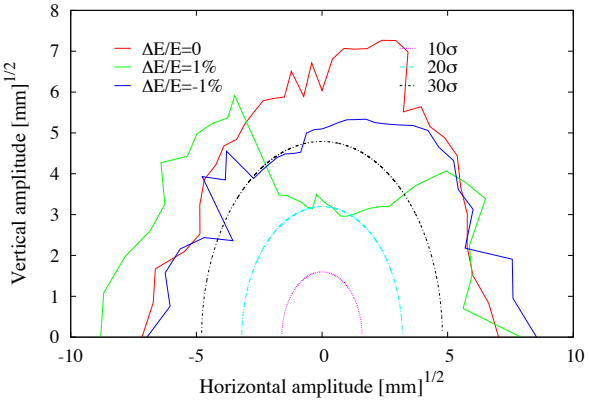

FIGURE 5. Dynamic aperture. The solid lines correspond to the maximum stable initial amplitude for energy offsets of 0 and $\pm 1\%$ over 1000 turns. The horizontal, vertical and synchrotron tunes are as shown in Table 1 for 5.289GeV. The dashed lines are the amplitudes for 10, 20, $30\sigma_x$, where σ_x assumes $\epsilon_x = 25.5$ nm-rad.

FIGURE 6. L0

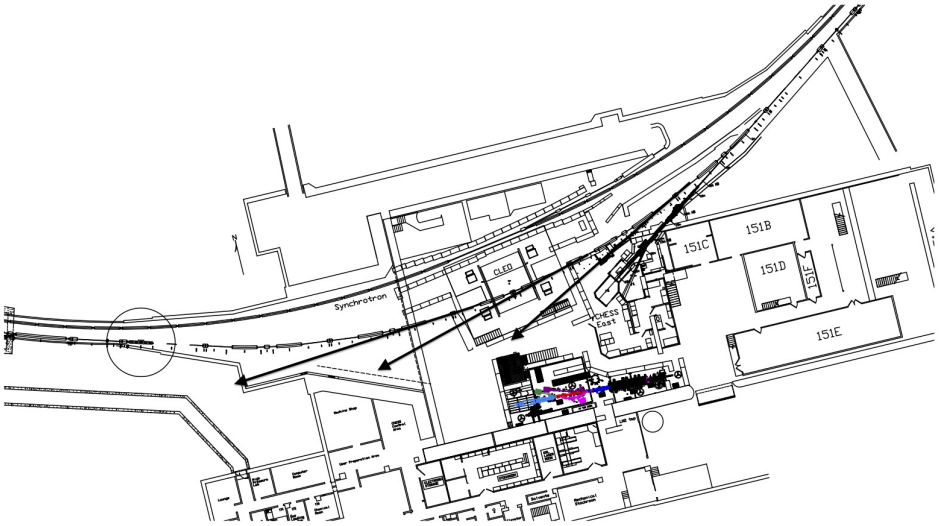

FIGURE 7. L0

emittance. The distortion of the bunch phase space complicates the interpretation of IBS measurements. The new layout would provide an opportunity to measure collective effects with significantly smaller emittance, (both transverse and longitudinal) and where there is no distinction between normal mode and projected emittance. Of course to fully exploit the capability of CESR for investigation of ultra-low emittance beams, it is essential that we preserve the capability to circulate positrons. To that end, we should give serious consideration to the possibility of coating the entire CESR vacuum chamber with TiN to mitigate the effect of the cloud for operation with positrons for CHESS.

On the time scale of the upgrade, the study of electron cloud model parameters and mitigations will have been completed. (Do we need to preserve the experimental test regions at 15E/W?) Perhaps we can instrument one of the hard bends or x-ray beam size measurement ? Alternatively, we might install a dedicated, short wiggler magnet in L3 as a source of x-rays for an xBSM. We presently have visible light beam size monitors in L3 for both electrons and positrons. The source of the synchrotron radiation is the soft bend. Horizontal beam size is measured with accuracy of a few percent. Our ability to measure vertical beam size using the vertically polarized component of the light is limited due to the relatively low field of the soft bend. If the hardbend-softbend pair is replaced with a normal bending magnet, the vBSM could serve to measure vertical as well as horizontal size.

10. Injection

As the circumference of the storage ring is preserved in the new configuration, no modification of injector chain, extraction kickers, or pulsed elements is required.

11. Magnet Modifications - Hard bends

We consider the introduction of gradient into the hard bends via a current sheet. We imagine a sheet with 5 mm thickness estimate power and the cost of the copper. The power dissipated in a single coil is

$$P = \frac{L}{w \cdot t}\rho I^2$$

where the L is twice the length of the magnet, w and t are with width and thickness of the conductor, ρ is the resistivity of copper. Of course if we can manage to double the thickness of the conductor to 10 mm, we reduce the power by 2. From Alexander's calculation we relate gradient and current

$$G = \frac{0.8\pi I_0}{wg} \rightarrow I_0 = \frac{wg}{0.8\pi}G$$

where w is the width of the current sheet and g the pole gap. The gradient at 6.5 GeV is 2.28 kG/cm and the current is 10.6 kA assuming a 6.5 cm gap and conductor width of 18cm.

Table 2. Dipole and quadrupole magnet parameters

Parameter	Hard bend	Quad(100cm)
k[m^{-2}]	-0.1056	0.78
gradient[T/m](@6.5GeV)	2.28	1.69
length[m]	3.238	92
width[m]	0.18	0.0058
thickness[m]	0.005	0.0058
density[kg/m^3]	8940	8940
Mass/magnet [kg]	43.4	221
Cost[$/kg]	6.60	6.60
Turns	18	80/pole
Current [A-turns]	10600	9760
Current/turn [A]	590	122
Current density [A/mm^{-3}]	11.8	3.68
Resistivity [ohms-m]	1.7×10^{-8}	1.7×10^{-8}
Power/magnet [kW]	27	5388
Total copper [$]	344	1459

The 11.8 A/mm^3 current density is beyond the capacity of copper. Again, if we double the thickness of the copper to 1cm, current density is 5.9 A/mm^3 which is probably manageable with water cooling.

11.1. **Magnets.**

11.1.1. *Quadrupoles.* We assume that new quadrupole coils are purchased for the 6.5GeV CHESS upgrade and that there will be negligible additional materials required to add laminations to lengthen 5 60cm quads to 100cm. (Let's include the coils for the 100cm quad in our order for the new coils for the 60cm quads.)

TABLE 3. Quadrupole parameters

Length	60cm	100cm
Conductor	$\frac{1}{4}^{"} \times \frac{1}{4}^{"}$ bare	
Cooling hole diameter[inches/mm]	0.125/3.175	0.125/3.175
Area of conductor[in^2/mm^2]	0.05138/33.15	0.05138/33.15
Number of turns	40	40
Length of water channel[ft/m]	178.9/ 60	301.84/92
Resistivity[Ω]	0.0305	0.0468
Maximal current[A][1]	385	
Maximal A-turns	16940	
Power dissipation@100A[W]	305	468
Pressure drop[psi]	50	50
Water flow rate[cm^3/s]	10	8.07
Temperature gain[C]	20	20
Power carried out by water[W]	835	674
Quad strengh k [m^{-2}]	0.7	0.78
Gradient@6.5GeV [kG/cm]	1.73	1.69
Gradient/per coil[kG/cm]	0.865	0.845
Coil current [A]	125	122
Total gradient(two coils)[kG/cm]	1.73	1.69
Total Power dissipated[W/coil]	477	696
Voltage/coil	3.813	5.71
Total voltage[V]	30.504	45.68

11.1.2. *Dipoles.* We consider two possibilities for upgrading the dipoles.

(1) The existing dipoles are machined for the appropriate gradient and reworked with 35m radius or
(2) The magnets are replaced. Based on the costing of ERL magnets in 2010, we estimate that the cost of building new hard bend magnets, iron and coil, at \$50k/magnet or \$500k total for 10.

[1] 7500A/sq.in maximum for water cooled Copper

11.1.3. *Power supplies.* We assume that new power supplies will be required for the nine quadrupoles (4-60cm and 5-100cm) described in Table 4, that the dipole and corrector magnets run off of the existing supplies. To drive the high current choppers, an

TABLE 4. Quadrupole parameters

Quadrupole	60cm	100cm
Voltage[V]	30.504	45.68
Current[A]	125	122
Chopper rating[A]	300	300
Unit cost[$]	10k	10k
Total cost [$]	40k	50k

additional quad buss supply will be required at a cost of about $70k. Total cost for magnet power supplies is $160k.

11.2. **Vacuum chambers.** We estimate that there are more than 250 ft of extrusions in the warehouse, sufficient to replace all of the chambers through L0. We will use distributed pump power supplies. Beam position monitors, flanges, distributed pumps, lumped pumps are new as shown in Table 5. The cost of coating with TiN for electron cloud mitigation is not included.

11.3. **Total cost.** See Table 6. We have assumed new dipole magnets and new magnet stands with pricing for both based on the 2009 ERL costing study and some adjustment for inflation. The cost of modifying the existing hard bends and building our own stands is likely less than half that of new equipment. The estimate for new quadrupole coils is determined as twice the cost of the copper. In practice, the new coils will be paid for as part of the CHESS high energy upgrade.

12. PENULTIMATE CESR

The reconfiguration of the hard bend region described above can be the basis of a global upgrade of the storage ring. By extending the conversion of single function to combined function magnets for all of the ring dipoles, we reduce the horizontal emittance at 5GeV (for x-ray operation) to $\sim$ 1nm-rad and at 2GeV (damping ring studies) to less than 80 pm-rad, well into the parameter space of the world's most brilliant x-ray sources and ambitious positron sources. The concept is to split the arc dipoles that are now paired with a single coil to form a 6.6 m chevron, into two 3.3m rectangular bends, and then to modify the poles

[2]Cost is fixtures for bending to 35m radius and cutting pump slots

[3]Cost is for fixtures to prepare extrusions, remove pump chamber, etc.

[4]Assuming new magnets, based on estimate from 2010 ERL costing

[5]Estimated as twice the cost of the copper for 10 100cm quadrupoles

[6]From ERL costing study

TABLE 5. Vacuum system

Component	Number	Cost/item[$]	Total Cost [$]
Bend chamber [2]	10	10k	10k
Quadrupole chamber fixtures[3]	10	10k	10k
Wiggler chambers	6	use existing chambers	
Undulator chambers	6	0	0
Flanges (2/chamber)	32	2.5k	80k
Distributed pumps	10	3k	30k
Undulator crotches	5	5k	50k
Wiggler positron absorber	6	5k	30k
Lumped pumps	10	8k	80k
BPM	15	6k	90k
sliding joints	5	10k	50k
gate valves	2	use existing inventory	
ccg	5	2k	10k
rga	2	20k	40k
Ozonator	1	8k	8k
Bakeout supplies	1	10k	10k
TiN coating	10		
Other M&S	1	10k	10k
Total			508k

TABLE 6. Total cost

Component	Cost [k$]
Bend magnets[4]	500
Quadrupole Power supplies	160
Quadrupole Coils[5]	27
Vacuum system	508
Dipole Magnet stands[6]	150
Quadrupole Magnet stands	25
Corrector magnets	100
Total	1470

to include both horizontal de-focusing, quadrupole and sextupole components. The arc cell is shown in Figure 10. A first order approximation of the optics of the ring-wide layout is shown in Figure 8. The dynamic aperture at 5.3GeV is shown in Figure 9 where the vertical chromaticity is compensated by the sextuple component of the combined function bends and the horizontal chromaticity by the sextupole adjacent to the quadrupole. Note that all quadrupoles are horizontally focusing. The layout shown in Figure 8 is a simplification insofar as there is no zero dispersion straight for the damping wigglers that now exist in

the ring arcs, and there is no match to the injection lines. Parameters of the "Penultimate CESR" ring are shown in Table 7 for various beam energies.

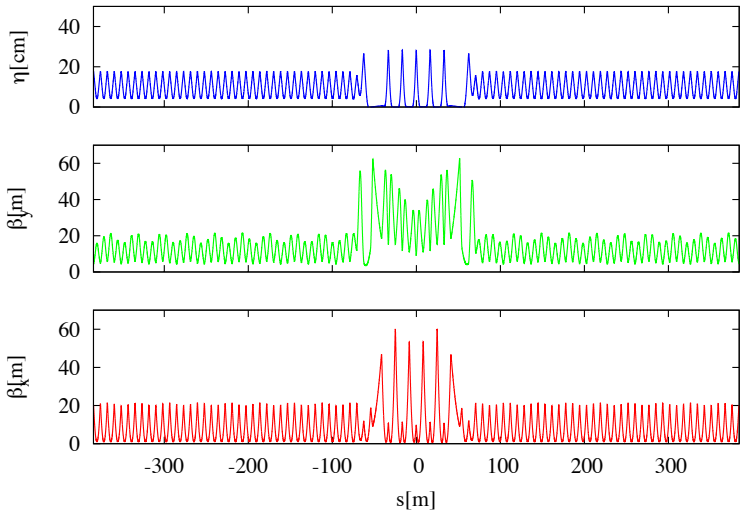

FIGURE 8. Penultimate CESR optics. The L0 region is here in the center of the figure.

The proposed reconfiguration of the full ring requires splitting the existing "chevron" bend magnets, modification of the magnet poles to include gradient and sextupole, and construction of new coils compatible with the shorter length. The quadrupoles can be reused as is. The sextupole magnets have only about 85% of the strength required to compensate chromaticity at 5.3 GeV. Some modification of the poles, and/or coils might coneivably suffice. Alternatively, additional sextupoles can be added to the opposite side of the quadrupole. The vacuum chambers would need to be rebuilt.

The magnet count in the reconfigured ring is summarized in Table 8

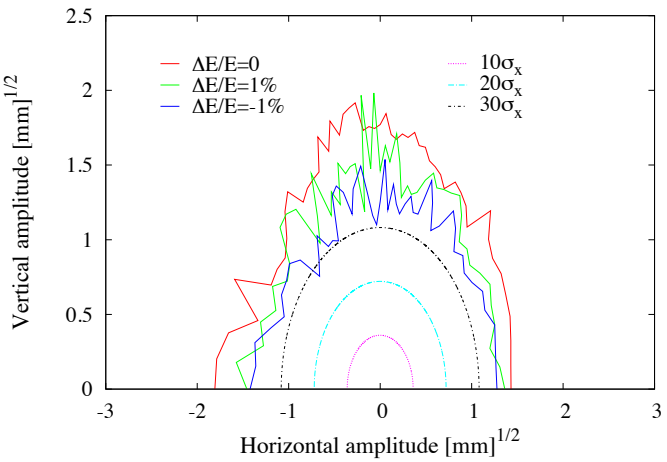

FIGURE 9. Penultimate CESR dynamic aperture. Lines indicate maximum initial amplitude that survives more than 1000 turns.

TABLE 7. Lattice parameters for Penultimate CESR. Note that (Beam Power [kW]) = (Energy Loss/Turn[MeV]) X (Beam Current [mA]) where Beam Power refers to the synchrotron radiation power only.) For beam energies 5.289 and 6.5 GeV, the lattice includes 6, 1m long, 1.1T undulators. For 3.0 and 2.1 GeV, numbers in parenthesis include damping wigglers.

Energy[GeV]	5.289	3.0	6.5	2.1
ϵ_x[nm-rad]	1.2	0.43(0.160)	1.9	0.21(0.075)
ϵ_y[pm-rad]	1	1(1)	1	1(0.5)
Current [mA]	300	500	150	500
Bunches	600	600	600	600
Q_x	35.13	35.13	35.13	35.13
Q_y	11.29	11.29	11.29	11.29
Q_z	0.01	0.0134	0.0091	0.016
Acc. Voltage [MV]	6	6	6	6
τ_x[ms]	11.1	66(23)	6.1	197(67)
τ_y[ms]	16.1	100(27)	9.0	297(75)
τ_z[ms]	10.4	67(14)	5.9	199(40)
$\alpha_p[\times 10^{-4}]$	4.36	4.36	4.36	4.36
$\sigma_E/E[\times 10^{-4}]$	8.2	4.4(9.6)	9.76	3.1(7.0)
σ_l[mm]	4.4	1.8(3.8)	5.7	1.0(2.3)
Energy loss/turn [MeV]	1.7	0.154(0.578)	3.7	0.036(0.142)
Beam Power [kW]	510	77(289)	555	18(71)

TABLE 8. Magnets for Penultimate CESR

Magnet	Number	Radius [m]	Gradient [m^{-2}]	Sextupole [m^{-3}]	length [m]
Arc Dipole	80	48.42	-0.103	-2.52	3.29
Hard bend	10	35.97	-0.106	0	3.238
Quadrupole[60cm]	89	-	0.82	-	0.6
Quadrupole[100cm]	5	-	0.78	-	1.0
Sextupole	78	-	-	18.0	0.272

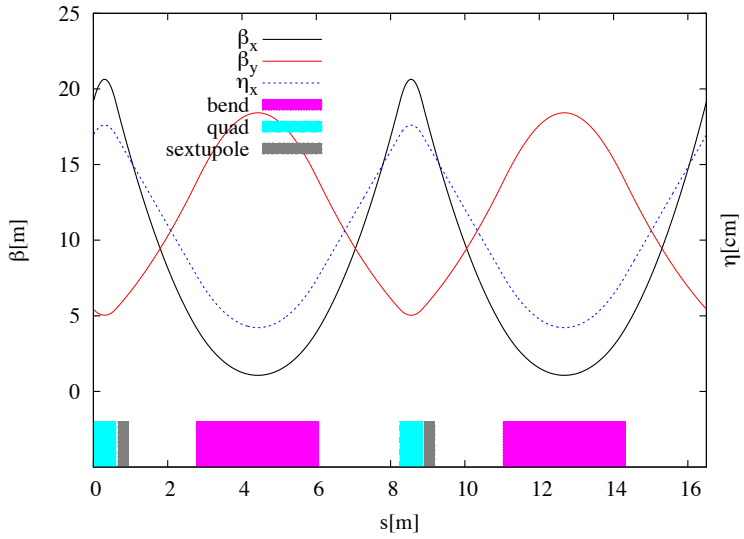

FIGURE 10. Ultimate CESR optics arc cell. The bend magnet includes vertically focusing quadrupole and sextupole components. The quadrupole and sextupole are both horizontally focusing.